On the simultaneous inference of susceptibility distributions and intervention effects from epidemic curves

Ibrahim Mohammed[a,b], Chris Robertson[a,c], M. Gabriela M. Gomes[a,d,*]

[a]*Department of Mathematics and Statistics, University of Strathclyde, Glasgow, G1 1XH, UK*
[b]*Department of Mathematical Sciences, Abubakar Tafawa Balewa University, Bauchi, Nigeria*
[c]*Public Health Scotland, Glasgow, G2 6QE, UK*
[d]*Centre for Mathematics and Applications (NOVA MATH), NOVA School of Science and Technology, Caparica, 2829-516, Portugal*

Abstract

Susceptible-Exposed-Infectious-Recovered (SEIR) models with inter-individual variation in susceptibility or exposure to infection were proposed early in the COVID-19 pandemic as a potential element of the mathematical/statistical toolset available to policy development. In comparison with other models employed at the time, those designed to estimate the effects of such variation fully tended to predict small epidemic waves and hence require less containment to achieve the same outcomes. However, these models never made it into mainstream COVID-19 policy making due to lack of prior validation of their inference capabilities. Here we report the results of the first systematic investigation of this matter. We simulate datasets using the model with strategically chosen parameter values, and then conduct maximum likelihood estimation to assess how well we can retrieve the assumed parameter values. We recommend fitting multiple epidemics with shared parameters to ensure identifiability.

Keywords: individual variation, epidemic model, parameter estimation, identifiability

1. Introduction

Susceptible-Exposed-Infectious-Recovered (SEIR) models are used extensively to study epidemics and guide public health policies. These models range in detail, from

---

*Corresponding author: gabriela.gomes@strath.ac.uk

simple systems of ordinary differential equations (ODEs), to higher-dimensional implementations that include disease progression, age structure, and other forms of heterogeneity Diekmann et al. (2013). Metapopulation Keeling and Rohani (2002) or agent-based models Kerr et al. (2021) are most commonly used when explicit descriptions of spatial connectivity are desired, although they also enable the representation of other heterogeneities such as person-to-person variability as stylised by Ayabina et al. (2025).

During the COVID-19 pandemic, several authors highlighted the significant role of individual variation in susceptibility and exposure to infection in flattening epidemic curves Britton et al. (2020); Neipel et al. (2020); Rose et al. (2021); Tkachenko et al. (2021); Montalbán et al. (2022); Gomes et al. (2022). However, despite being understood for decades McKendrick (1940); Gart (1968, 1972); Ball (1985); Katriel (2012), these ideas were treated with caution among scientific advisors to governments Wood et al. (2025) due to supposed parameter identifiability issues. Here we report the results of a thorough investigation of parameter identifiability in SEIR models.

We use SEIR models with individual variation in susceptibility to infection proposed by Montalbán et al. (2022); Gomes et al. (2022) during the pandemic. These models include non-pharmaceutical interventions (NPIs) as required, which also tend to flatten epidemic curves and be potentially confounded with heterogeneity in susceptibility. To test our ability to attribute flattning of epidemic curves correctly to heterogeneity or NPIs we generate synthetic epidemic datasets by simulating stochastic versions of those models. Then we perform sets of statistical inferences by fitting homogeneous and heterogeneous versions of the models to the simulated data. Model parameters are estimated by maximum likelihood.

In our study setup, we find that models that allow susceptibility to vary among individuals are able to infer that the coefficient of variation (CV) is negligible when fitting a dataset generated by a homogeneous model with NPIs. All other parameters are also accurate. By applying the Akaike information criterion (AIC), we obtain similar scores for homogeneous and heterogeneous models when the datasets are generated under the homogeneity assumption. By contrast, when the datasets are generated with inter-individual variation in susceptibility, homogeneous models overestimate the impact of NPI as misattribution of the effects of heterogeneity. AIC scores are noticeably lower for homogeneous models in these scenarios.

In addition to assessing the accuracy of the estimated parameters, we noticed some strong correlations between parameters. This was irrespective of whether models accounted for individual variation or not. To generate further insight, we varied the initial number of infectious individuals (seed) as to gain control over the stage

of the epidemic at the point of NPI introduction, we developed a scheme to fit two epidemic curves with different seeds (akin metapopulation modelling Ayabina et al. (2025)), and conducted profile likelihood analyses extensively. We conclude that two-epidemic fittings (as performed in Gomes et al. (2022)) are an effective strategy for reducing parameter correlations, and hence overcoming identifiability issues, overall.

2. Mathematical models

2.1. SEIR models with inter-individual variation in susceptibility

We adopt an SEIR model previously analysed by Montalbán et al. (2022) and applied to the COVID-19 pandemic by Gomes et al. (2022). Inter-individual variation in susceptibility to infection is incorporated as a multiplicative factor, x, of the rate of infection. The model is written in terms of differential equations as

$$
\begin{aligned}
\frac{\mathrm{d}S(x)}{\mathrm{d}t} &= -x\ c(t)\ \beta\ (\rho\ \mathsf{E} + \mathsf{I})\ \frac{S(x)}{\mathsf{N}}, \\
\frac{\mathrm{d}\mathsf{E}}{\mathrm{d}t} &= x\ c(t)\ \beta\ (\rho\ \mathsf{E} + \mathsf{I})\ \frac{S(x)}{\mathsf{N}} - \delta\ \mathsf{E}, \\
\frac{\mathrm{d}\mathsf{I}}{\mathrm{d}t} &= \delta\ \mathsf{E} - \gamma\ \mathsf{I},
\end{aligned}
\tag{1}
$$

where $S(x)$ represents the density of susceptible individuals as a function of the susceptibility factor x, $\mathsf{E} + \mathsf{I}$ is the number of individuals who have been exposed and are infected (accounting for an early stage of lower infectiousness, E). The recovered number R is derived from the conservation of total population size, $\mathsf{S} + \mathsf{E} + \mathsf{I} + \mathsf{R} = \mathsf{N}$, where $\mathsf{S} = \int S(x)\ \mathrm{d}x$. The main parameters are the average effective contact rate β, the rate of progression from E to I (assumed $\delta = 1/5.5$ per day (McAloon et al., 2020; Lauer et al., 2020)), the rate of removal from I (assumed $\gamma = 1/4$ per day (Nishiura et al., 2020; Li et al., 2020)) and the reduced infectiousness while in E (assumed $\rho = 0.5$). An additional time-dependent parameter $c(t)$ is included, which has a default value of 1 and will be used to study the effect of interventions. The basic reproduction number is given by

$$
\mathcal{R}_0 = \beta \left(\frac{\rho}{\delta} + \frac{1}{\gamma} \right).
\tag{2}
$$

Initial conditions for variables $S(x, t)$, $\mathsf{E}(t)$, $\mathsf{I}(t)$ are defined as to satisfy $S(x, 0) = (1 - 3.5\ \epsilon)\ q(x)\ \mathsf{N}$, $\mathsf{E}(t) = 2.5\ \epsilon\ \mathsf{N}$ and $\mathsf{I}(t) = \epsilon\ \mathsf{N}$ (see Supplementary material Section S1 for justification), where $q(x)$ is a probability density function with mean 1 and

coefficient of variation

$$\nu = \sqrt{\int (x-1)^2 q(x) dx}. \tag{3}$$

Following Novozhilov (2008), Montalbán et al. (2022) showed that when $q(x)$ is a gamma distribution, system (1) can be reduced exactly to

$$\begin{aligned}
\frac{d\mathsf{S}}{dt} &= -c(t)\ \beta\ (\rho\ \mathsf{E} + \mathsf{I})\ \left(\frac{\mathsf{S}}{\mathsf{N}}\right)^{1+\nu^2}, \\
\frac{d\mathsf{E}}{dt} &= c(t)\ \beta\ (\rho\ \mathsf{E} + \mathsf{I})\ \left(\frac{\mathsf{S}}{\mathsf{N}}\right)^{1+\nu^2} - \delta\ \mathsf{E}, \\
\frac{d\mathsf{I}}{dt} &= \delta\ \mathsf{E} - \gamma\ \mathsf{I},
\end{aligned} \tag{4}$$

The gamma distribution was described by Rose et al. (2021) as a "natural choice to account for variations in susceptibility" as it is the limiting distribution to which other initial distributions of susceptibility converge. This choice will be kept throughout this paper, although the treatment of the explicit system (1) can be replicated for any distribution while the use of the reduced version (4) is specific to gamma distributed susceptibility. In either formulation, the classical SEIR model is retrieved by setting $\nu = 0$.

Previous studies, including those by Novozhilov (2008); Neipel et al. (2020); Gomes et al. (2022); Montalbán et al. (2022); Rose et al. (2021), have demonstrated that heterogeneity in susceptibility reduces epidemic sizes. This occurs because highly susceptible individuals and infected first and hence selected out of the susceptible pool, a dynamic not captured by the classical homogeneous model. This effect is illustrated in Figure 1 (top). For example, around 50% of the population is expected to be infected over the course of an outbreak when CV is $\nu = \sqrt{2} \approx 1.414$. By comparison, when a homogeneous model is assumed ($\nu = 0$) the expected infected percentage rises to around 90%. In the bottom panel, corresponding trajectories for incidence of infection (represented as $\delta\ \mathsf{E}$) are shown, highlighting the higher peak in the absence of individual variation.
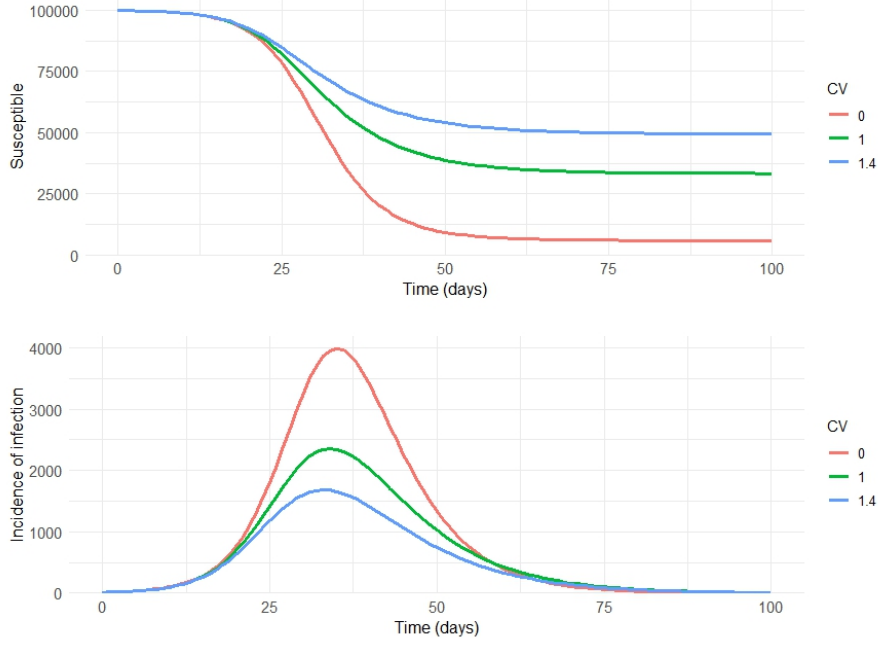
4

Figure 1: Dynamics of infection under the heterogeneous susceptibility SEIR model for different values of ν (bottom). The homogeneous SEIR model corresponds to $\nu = 0$. The top figure shows how the dynamics of the susceptible pool size changes with ν.

2.2. Non-pharmaceutical interventions (NPIs)

Outbreak awareness triggers, to some extent, a reduction in contract rates. This may be due to voluntary precautions or restrictions imposed by governments. To incorporate the effects of these co-called non-pharmaceutical interventions (NPIs) we use a time dependent factor $c(t)$ such as

$$c(t) = \begin{cases} 1, & \text{if } 0 < t \le t_0 \\ 1 - (1 - c_1)\dfrac{t - t_0}{t_1 - t_0}, & \text{if } t_0 < t \le t_1 \\ c_1, & \text{if } t_1 < t \end{cases} \tag{5}$$

where $0 \le c_1 \le 1$. This is profiled in Figure 2, with t_0 representing the time when contact rates begin to decrease and t_1 marking the beginning of maximal containment (such as lockdown).

When $c_1 < 1$, the dynamics of the susceptible numbers and the incidence of infection for a homogeneous model are affected as shown in Figure 3. It is clear that
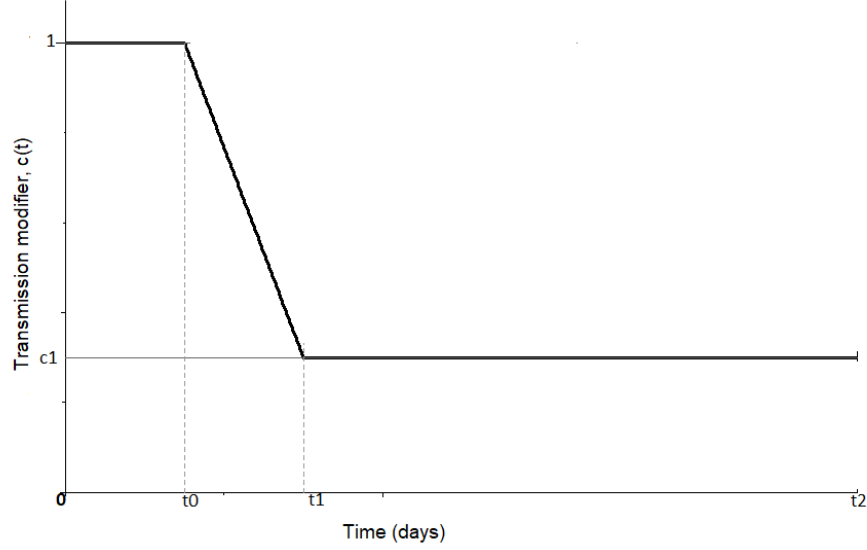
Figure 2: Schematic illustration of the factor $c(t)$, representing the combined effects of adaptive behavioural changes and NPIs on transmission.

both heterogeneity in susceptibility and NPIs flatten epidemic curves although for the specific NPI profiles adopted here the flattened curves have distinctive shapes.

A description of all the model parameters is provided in Table 1.

Table 1: Description of model parameters.

| Parameter	Description	Value
δ	Rate of progression from E to I	1/5.5 per day
γ	Rate of removal from I	1/4 per day
ρ	Infectiousness in E (relative to I)	0.5
$\mathcal{R}_0$	Basic reproduction number	Variable
ν	Coefficient of variation in susceptibility	Variable
c_1	Maximal reduction in transmission by NPIs	Variable
t_0	Time to beginning of behavioural change	15 days
t_1	Time to beginning of lockdown	20 days

6
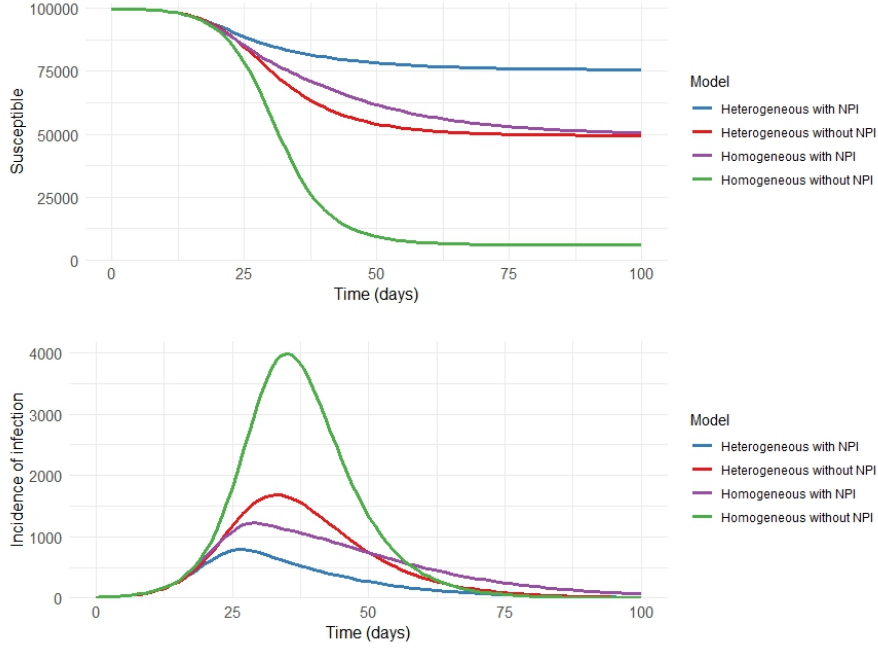
Figure 3: The combined effects of heterogeneity in susceptibility and NPIs on epidemic trajectories for different values of ν and constant NPI $c_1 = 0.4$ (bottom). The homogeneous SEIR model corresponds to $\nu = 0$. The top figure shows how the susceptible pool changes with both ν and c_1.

3. Simulations

We aim to identify the effects of individual variation and NPIs on epidemic trajectories based on a given epidemic dataset affected by both. We design a systematic study with four different incidence time series generated as follows:

1. Homogeneous model ($\nu = 0$) without NPIs ($c_1 = 1$).
2. Heterogeneous model ($\nu > 0$) without NPIs ($c_1 = 1$).
3. Homogeneous model ($\nu = 0$) with NPIs ($c_1 < 1$).
4. Heterogeneous model ($\nu > 0$) with NPIs ($c_1 < 1$).

The datasets are generated by running model (4), with NPIs as in (5). We define incidence of infection as $\delta\,\mathsf{E}$ and adopt a Poisson error structure to obtain the time series

$$y(t) \sim \text{Poisson}(\hat{\imath}(t)) \quad \text{for each day } t \in \mathbb{N}.$$

For each combination of parameters, 200 datasets are simulated and we fit both the homogeneous model (to estimate $\mathcal{R}_0$, t_0 and c_1) and the model with heterogeneity

represented by parameter ν (to estimate $\mathcal{R}_0$, ν, t_0 and c_1), while keeping other parameters constant as in Table 1.

4. Maximum likelihood estimation

With the heterogeneous susceptibility models, we estimate two sets of parameters from the datasets described in the previous section:

$$\boldsymbol{\theta_a} := (\mathcal{R}_0, \nu) \tag{6}$$

$$\boldsymbol{\theta_b} := (\mathcal{R}_0, \nu, t_0, c_1). \tag{7}$$

The first case corresponds to estimating $\boldsymbol{\theta_a}$ by fitting the models with no NPIs to the first two datasets in Section 3. This is to establish how well heterogeneity can be estimated in the absence of the potentially confounding effects of interventions, and to test how reliable the heterogeneous susceptibility model is at estimating "no variation" when the dataset has been generated by the homogeneous model.

The second case of interest is estimating $\boldsymbol{\theta_b}$ from the last two datasets in Section 3. But we shall also estimate $\boldsymbol{\theta_b}$ from the other datasets to test whether how well models identify when there is "no intervention".

Let $x_1, x_2, ..., x_n$ be the model simulation of the observations for the time series epidemic data $y_1, y_2, ..., y_n$. Let $f(y_1, y_2, ...y_n | x_1, x_2, ..., x_n, \boldsymbol{\theta})$ be the joint density function which defines a probability distribution for each value of a parameter vector $\boldsymbol{\theta} := \boldsymbol{\theta_a} \cup \{\rho, \delta, \gamma, t_1\}$ or $\boldsymbol{\theta} := \boldsymbol{\theta_b} \cup \{\rho, \delta, \gamma, t_1\}$.

The likelihood function is the density function evaluated at the data which is defined as

$$\mathcal{L}(\boldsymbol{\theta}) := \prod_{i=1}^{n} f(y_i | x_i, \boldsymbol{\theta}).$$

It is usually convenient to work with the log-likelihood function given by

$$l(\boldsymbol{\theta}) := \log \mathcal{L}(\boldsymbol{\theta}) = \sum_{i=1}^{n} f(y_i | x_i, \boldsymbol{\theta}). \tag{8}$$

Parameter estimation was performed in Rstudio by maximizing the log-likelihood function (8) of observing the simulated data $\{y_1, y_2, ..., y_n\}$ given the model, and its parameters.

5. Baseline analysis

This section is entirely devoted to presenting and discussing the results of a detailed parameter estimation study for a representative choice of parameters. We group the datasets described in Section 3 into two broad cases:

I : Epidemic datasets simulated from the homogeneous model ((4) with $\nu = 0$) and $\mathcal{R}_0 = 3$, which are further classified as datasets without intervention ((a) $c_1 = 0$) and with intervention ((b) $c_1 = 0.3$).

II : Epidemic datasets simulated from heterogeneous susceptibility ((4) with $\nu = 1.414$) and $\mathcal{R}_0 = 3$, which are also classified as datasets without intervention ((a) $c_1 = 0$) and with intervention ((b) $c_1 = 0.3$).

As outlined in Section 4, we then estimate parameter combinations $\boldsymbol{\theta_a} := (\mathcal{R}_0, \nu$ or $\boldsymbol{\theta_b} := (\mathcal{R}_0, \nu, t_0, c_1)$ from the simulated the datasets. Table 2 shows the resulting summary statistics which are discussed in the remaining of this section. We refer to this as the "baseline analysis" as it provides a basis for later sections which either deepen the study or extended it by modifying conditions stipulated here.

Table 2: Summary results for parameter estimates and 95% confidence intervals.

Case	Parameter estimates and 95% CI for both Heterogeneous and **Homogeneous** (**bold face**) models				
	$\mathcal{R}_0$	ν	t_0	c_1	AIC
I (a) (i)	3.00 (2.99, 3.01)	0.029 (0.00, 0.33)	NA	NA	817.23
	3.00 (3.00, 3.01)	NA	NA	NA	**815.58**
I (a) (ii)	3.00 (2.99, 3.03)	0.0 (0.00, 4.9e219)	0.1 (0.00, 4.6e12)	0.997 (0.98, 1.00)	805.71
	3.00 (2.99, 3.00)	NA	**0.00 (0.00, 1.05e79)**	**0.999,(0.784, 1.00)**	**808.03**
I(b)	3.00 (2.97, 3.04)	0.201 (0.04, 0.912)	14.9 (14.30, 15.60)	0.302 (0.296 , 0.308)	794.73
	3.00 (2.97, 3.04)	NA	**15.0(14.4, 15.60)**	**0.30 (0.296, 0.304)**	**791.09**
II(a)(i)	3.00 (2.99, 3.01)	1.415 (1.40, 1.43)	NA	NA	814.67
	2.93 (2.92, 2.94)	**NA**	**NA**	**NA**	**30415.99**
II(a) (ii)	3.00 (2.98, 3.02)	1.411 (1.394, 1.426)	0.3 (0, 1.39e21)	0.995 (0.82, 1.00)	816.37
	2.74 (2.73, 3.00)	NA	**28.5,(28.3, 28.7)**	**0.352 (0.348, 0.355)**	**2132.95**
II(b)	3.00 (2.95, 3.05)	1.406(1.157, 1.768)	15.00 (14.4, 15.70)	0.299 (0.274, 0.331)	713.27
	2.94 (2.89, 3.00)	NA	**14.90 (14.3, 15.5)**	**0.24 (0.236, 0.243)**	**727.54**

5.1. Case I(a): Homogeneous datasets without NPIs

Illustrative fittings for this case are provided in Supplementary Figure S2. There are essentially two scenarios.

First, to simply test whether the heterogeneous susceptibility model correctly infers that the data had been generated by a homogeneous model, we conduct an analysis where fittings are conducted with models that do not include NPIs (so, only parameters $\boldsymbol{\theta_a}$ are estimated). This is to test for potential confounding issues between

$\mathcal{R}_0$ and ν. Table 2, Case I(a)(i), shows the summary statistics for the model-based parameter estimates. Both homogeneous and heterogeneous models make unbiased estimates of the basic reproduction number $\hat{\mathcal{R}}_0$ (3.00, with high precision), with the heterogeneous susceptibility model estimating a coefficient of variation $\hat{\nu}$ as 0.029 with 95% CI $(0.00, 0.33)$. The AIC scores from the table are 815.58 for homogeneous and 817.23 for heterogeneous, which are not significantly different.

Second, to exclude potential confounding issues between $\mathcal{R}_0$ and c_1, we use the same simulated datasets as in the first case, but fit them with a model that allows for NPI effects. Table 2, Case I(a)(ii), shows the summary statistics for the model-based estimates of parameters $\boldsymbol{\theta_b}$. Again, both homogeneous and heterogeneous susceptibility models make unbiased estimates of the basic reproduction number $\hat{R}_0$ (3.00, with high precision), with heterogeneous susceptibility also estimating a coefficient of variation $\hat{\nu}$ very precisely as 0.0. Furthermore, the NPI parameter, specified as $c_1 = 1$ in the simulation of the data, is estimated by both models to be very close to 1 (0.997 with 95% CI $(0.98, 1.00)$ for homogeneous, and 0.999 with 95% CI $(0.784, 1.00)$ for heterogeneous models), while the estimate for the time point when transmission begins to decrease $\hat{t}_0$ is estimated as a redundant parameter by both models with extreme confidence intervals. The AIC score is 805.71 and 808.03 for homogeneous and heterogeneous models, respectively, so again very similar.

5.2. Homogeneous datasets with NPIs: Case I(b)

This case is particularly informative given that both heterogeneity and NPIs have the effect of flattening epidemic curves and it is important that any such effects are attributed to the true cause. Illustrative fittings are shown in Supplementary Figure S3.

When we fit the simulated datasets with homogeneous and heterogeneous models with NPIs to estimate parameters $\boldsymbol{\theta_b}$, both models give similar estimates for the transmission parameters ($\mathcal{R}_0$, c_1, and t_0), which are unbiased as can be seen from Table 2, Case I(b), and Figure 4. The estimates based on the heterogeneous susceptibility (vs. homogeneous) model are $\hat{\mathcal{R}}_0 = 3.00$ (3.00), $\hat{c}_1 = 0.302$ (0.30) and $\hat{t}_0 = 14.90$ (15.0). The true value for CV is 0 but the heterogeneous model estimates a biased value $\hat{\nu} = 0.204$ with 95% CI $(0.04, 0.912)$, as clearly visible in the CV distribution in Figure 4. This bias reflects the confounding between NPIs and heterogeneity effects, which we address using the concurrent epidemic approach discussed in later sections. The AIC scores for the two models are similar, with 794.73 for heterogeneous susceptibility and 791.09 for the homogeneous model.

Moreover, from the correlation plots in Figure 5 we identify various correlations between parameters of both models suggesting potential issues with identifiability.
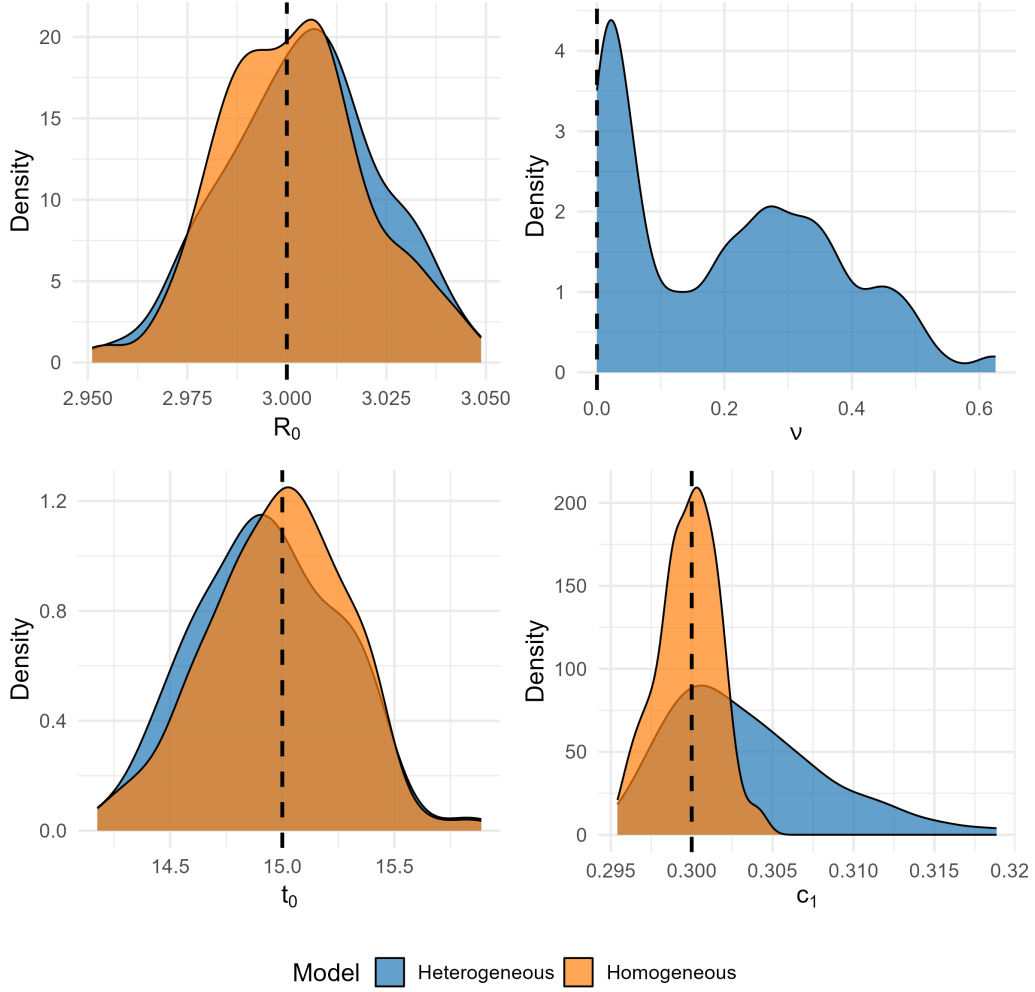
10

Figure 4: Distributions of the estimated parameters for Case I(b): Homogeneous data with impact of NPIs ($\mathcal{R}_0 = 3$, $c_1 = 0.3$, $t_0 = 15$ days). The blue fill represents estimates from the heterogeneous susceptibility model, while the orange fill represents those from the homogeneous model. Vertical dashed lines indicate the true specified parameter values. Both models accurately recover $\mathcal{R}_0$, t_0, and the value of the NPI parameter c_1, with the heterogeneous model correctly estimating negligible heterogeneity (coefficient of variation ν near 0).

5.3. Case II(a): Heterogeneous datasets without NPIs

Illustrative fittings for this case are provided in Supplementary Figure S4. Again there are two scenarios.
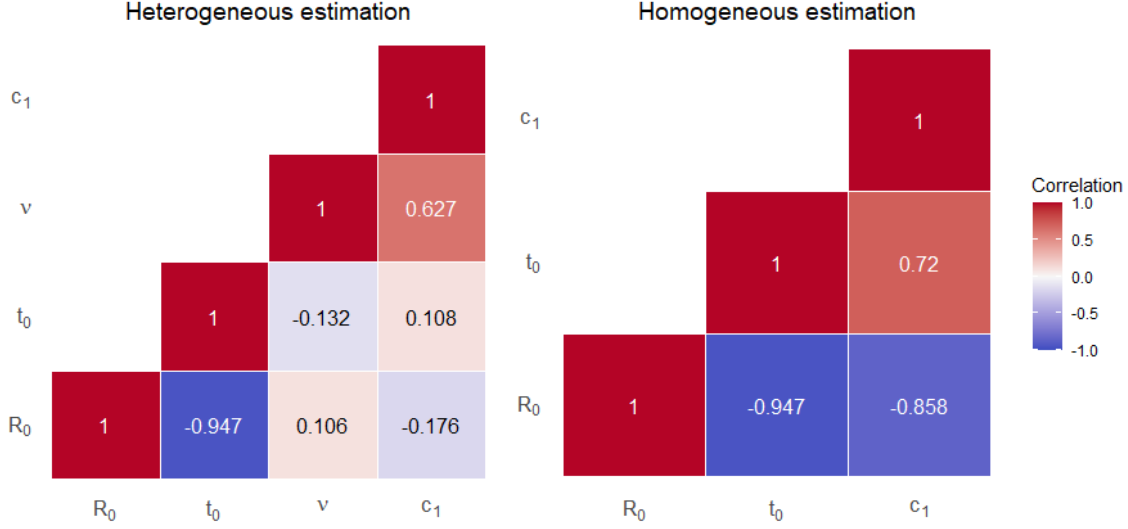
Figure 5: Median parameter correlation heatmaps for Case I(b): homogeneous data with impact of NPIs. Both heterogeneous (left) and homogeneous (right) models show very strong negative correlations between $\mathcal{R}_0$ and t_0 (-0.947).

First, recalling that heterogeneity in susceptibility flattens epidemic curves, we might expect that, once the dataset has been generated using a model that incorporated some degree of inter-individual variation, it should be very difficult for a homogeneous model to fit the data unless the lack of heterogeneity could be somehow compensated by a change in $\mathcal{R}_0$. But in Section 5.1 we did not detect any confounding between $\mathcal{R}_0$ and ν, suggesting that the homogeneous model may fail to provide adequate fits to heterogeneous data when NPIs are not allowed to be part of the inference. Table 2, Case II(a)(i), shows the summary statistics for the estimates of model parameters $\boldsymbol{\theta_a}$. The heterogeneous model recaptures the specified $\mathcal{R}_0$ and ν as 3.00 with 95% CI $(2.99, 3.01)$ and 1.415 with 95% CI $(1.40, 1.43)$, respectively, while the homogeneous model makes a biased estimate of the basic reproduction number $\mathcal{R}_0$ as 2.93 with 95% CI $(2.92, 2.94)$. The AIC scores from the table are 814.67 for heterogeneous susceptibility and 30415.99 for the homogeneous model, which are far from being close, an indication that the homogeneous model does not fit the data which is also seen very clearly from Figure S4.

Second, we fit the same simulated datasets with a model that allows for NPI effects. We might expect NPIs to provide a means to improve the fits attempted above at the expense of biasing estimates. Table 2, Case II(a)(ii), shows the summary statistics for the estimates of model parameters $\boldsymbol{\theta_b}$. The parameter estimates confirm that the heterogeneous susceptibility model effectively estimates the true $\hat{R}_0$ and $\hat{\nu}$ as 3.00 with 95% CI $(2.98, 3.02)$ and 1.411 with 95% CI $(1.394, 1.426)$ as well the impact of NPIs $\hat{c}_1 = 0.995$ (95% CI being $(0.82, 1.00)$) - an indication of no effects of NPIs. As for the homogeneous model, in addition to biased estimates of $\hat{R}_0$ as 2.74 with 95% CI $(2.73, 3.0)$, it also estimates that there was a strict NPI with $\hat{c}_1 = 0.352$ and 95% CI $(0.348, 0.355)$ and a non-existent parameter t_0 estimated with high precision ($\hat{t_0} = 28.5$ and 95% CI $(28.3, 28.7)$), thereby miss-attributing effect of heterogeneity to intervention. The AIC scores in this case are 818.07 for heterogeneous susceptibility and 2132.95 for the homogeneous model, again confirming the substantially better fit of the heterogeneous model.

5.4. Case II(b): Heterogeneous datasets with NPIs

Here we finally generate a datasets using the full heterogeneous model (4) and NPIs (5). We aim to estimate both the effect of heterogeneity and the impact of the NPIs from this data. Illustrative fittings are shown in Supplementary Figure S5.

The summary statistics for the estimates of model parameters $\boldsymbol{\theta_b}$ are also shown in Table 2, Case II(b), while Figure 6 shows the parameter distributions and mean estimates. For the homogeneous model, the basic reproduction number $\mathcal{R}_0$ has an estimate of 2.94 with 95% CI $(2.89, 3.00)$, and $\hat{t_0} = 14.90$ with 95% CI $(14.3, 15.5)$, slightly under the true value. Moreover, the impact of the NPIs with a mean estimate $\hat{c}_1 = 0.24$ at 95% CI $(0.236, 0.243)$ is also biased but enables the fitted model in Figure S5 to "match" the datasets.

On the other hand, the heterogeneous susceptibility model, as in the case of datasets with no impact of NPIs, accurately estimates the specified parameters as follows: $\hat{\mathcal{R}}_0 = 3.00$ with 95% CI $(2.95, 3.05)$, $\hat{\nu} = 1.406$ with 95% CI $(1.157, 1.768)$, the impact of NPIs $\hat{c}_1 = 0.299$ (95% CI being $(0.274, 0.331)$) and $\hat{t_0} = 15.0$ with 95% CI $(14.4, 15.70)$. Thus both impact of NPIs and heterogeneity are simultaneously estimated accurately.

In terms of the AIC, the heterogeneous model indicates a better fit to the data with a score of 713.27 than the homogeneous model which scored 727.54.

From the correlation plots in Figure 7, however, some strong correlations are apparent. The homogeneous estimation exhibits negative correlations between the estimates of t_0 and $\mathcal{R}_0$, and the estimates of t_0 and c_1. For the heterogeneous model, there is a positive correlation between the estimates of $\mathcal{R}_0$ and c_1, and the estimates
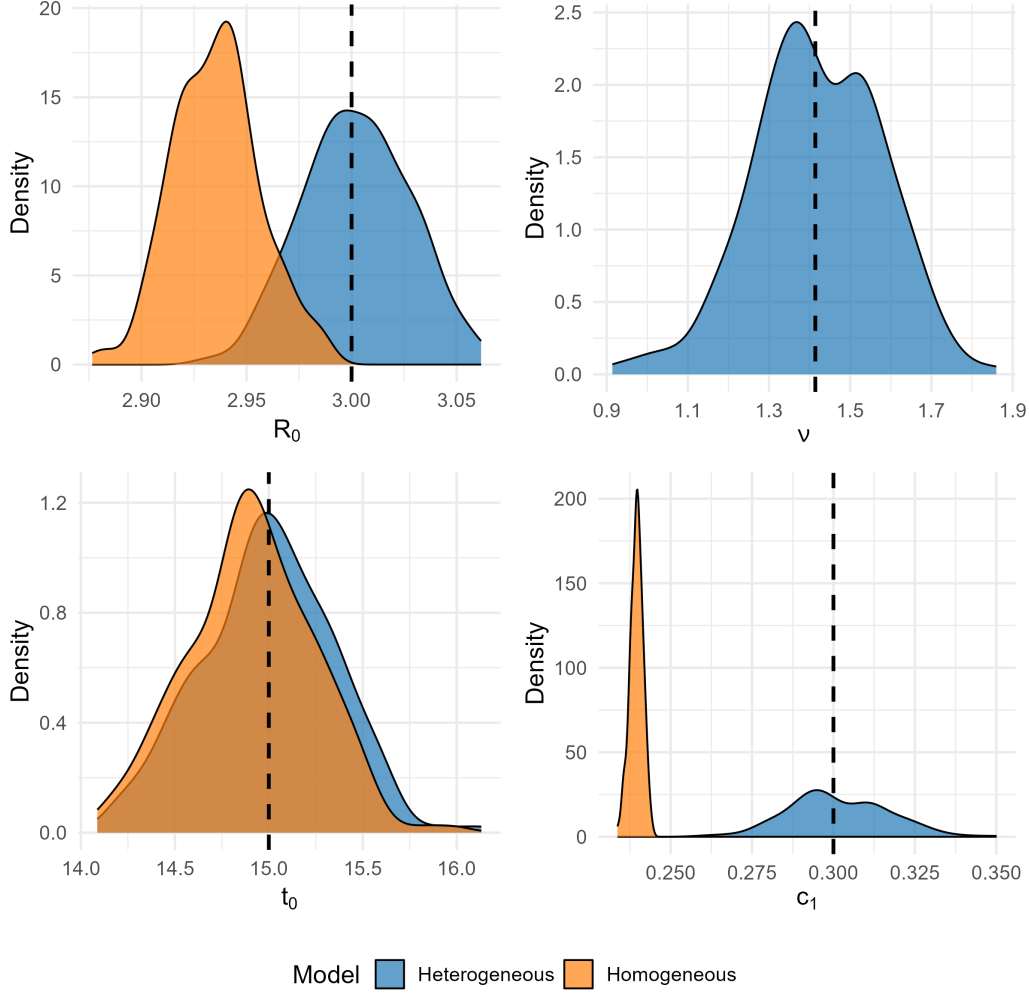
13

Figure 6: **Distributions of the estimated parameters for Case II(b): Heterogeneous data with impact of NPIs ($\mathcal{R}_0 = 3$, $\nu = 1.414$, $c_1 = 0.3$, $t_0 = 15$ days).** The blue fill represents estimates from the heterogeneous susceptibility model, while the orange fill represents those from the homogeneous model. Vertical dashed lines indicates the true specified parameter values. The heterogeneous model accurately recovers all parameters, while the homogeneous model underestimates $\mathcal{R}_0$, incorrectly estimates t_0, and underestimates the NPI parameter (predicting $c_1 \approx 0.24$ instead of the true value 0.3).

of ν and c_1, and also a negative correlation between the estimates of t_0 and $\mathcal{R}_0$. Overall, there are correlations in both model fits but the one that concerns us more here is the correlation of 0.974 between the impact of the NPIs and CV. This may

indicate non-identifiability of the parameters, although from our systematic study we know that, with the heterogeneous model, true values of the parameters have been estimated in all cases. In Supplementary Material Supplementary Section S3 we investigate how these results vary with the initial condition $I(0)$ and intervention strength parameter c_1.

To alleviate the correlation between the coefficient of variation ν and the impact of NPIs c_1, we will simulate concurrent epidemics, mimicking multiple areas of the same country (as in Gomes et al. (2022) for England and Scotland). Models will be fitted to these data simultaneously by maximizing the sum of the log-likelihoods from the individual epidemic datasets to estimate $\boldsymbol{\theta_b}$. This will be presented in the following sections.
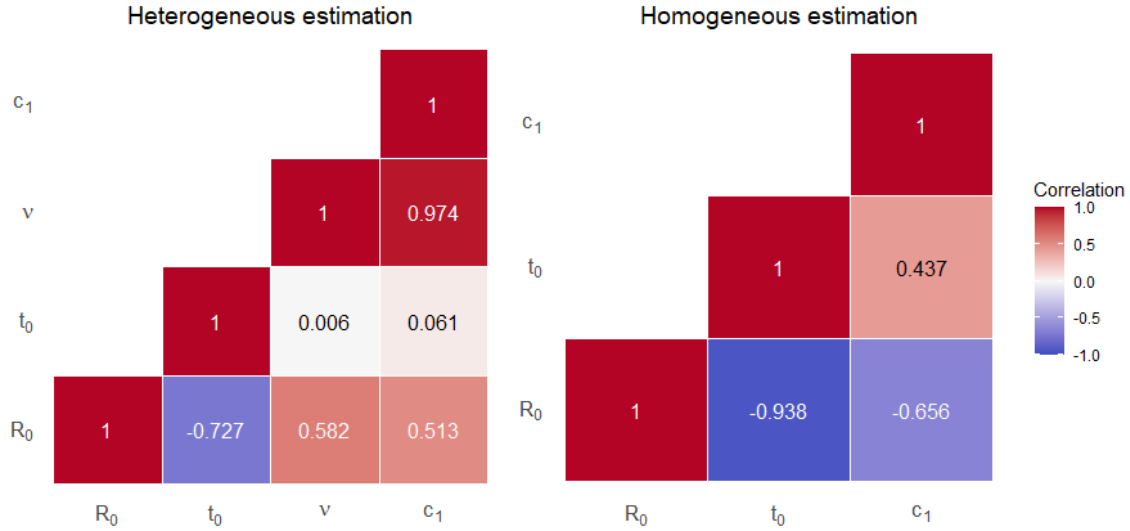

Figure 7: Median parameter correlation heatmaps for Case II(b): heterogeneous data with impact of NPIs. The heterogeneous model (left) shows a very strong positive correlation between ν and c_1 (0.974). The homogeneous model (right) shows a very strong negative correlations between $\mathcal{R}_0$ and t_0 (-0.938).

6. Profile likelihood analysis and parameter identifiability

As highlighted in Section 5, we have encountered correlations between the estimated parameters. Given our focus on individual variation in susceptibility, correlations that involve the coefficient of variation (ν) are of special interest (particularly those between ν with the non-pharmaceutical intervention parameter, c_1).

To address this problem, we draw on a simple yet powerful idea: different epidemic trajectories — arising from the same underlying disease parameters but differing in initial conditions — contain complementary information that can resolve the issues encountered in single-epidemic analyses. Consider two epidemics with identical values of $\mathcal{R}_0$, ν, t_0 and c_1, but different initial numbers of exposed and infectious individuals. Although governed by the same model, their distinct initial states lead to different observed trajectories. These differences act like independent "views" of the same parameter landscape, allowing us to distinguish the contributions of heterogeneity and intervention more effectively.

The key idea is that certain parameters "express" themselves differently under varying dynamical conditions. Particularly, in the epidemic with the larger number of people initially infected, heterogeneity would have acted for a longer period prior to intervention than in the other case. Hence, observing both helps the separation of the effects of heterogeneity and NPIs. More generally, by observing how the same parameters manifest across multiple epidemic contexts, we gain a better chance of correctly identifying their true values.

This intuition is supported by established results in the literature: when multiple independent datasets are analysed jointly, their Fisher information matrices aggregate (Anderson and Burnham, 2004; Lehmann and Casella, 2006). This improves the conditioning of the estimation problem and reduces the parameter correlations that drive identifiability issues. Such multi-dataset approaches are widely used in statistics and Bayesian inference to improve identifiability and reduce estimation uncertainty (Gelman et al., 2013; Robert and Casella, 1999).

This principle has already shown real-world success. For example, Gomes et al. (2022) fitted epidemic models jointly to COVID-19 data from England and Scotland and found that susceptibility heterogeneity could lower the herd immunity threshold to 25–29%, compared to 60–67% under homogeneity assumptions. Failing to account for heterogeneity might then lead to overestimation of epidemic severity and intervention needs.

In this section, we build on those insights by conducting the first systematic simulation-based investigation into how two-epidemic analyses can resolve identifiability problems inherent to single-epidemic inference discussed above. Our approach evaluates:

- whether analysing two concurrent epidemics improves identifiability of ν and c_1;

- whether such improvements are robust to different intervention strengths;

- and the degree to which estimation precision and parameter correlations are affected.

In the sections that follow, we present detailed profile likelihood and correlation analyses that demonstrate how this approach breaks the confounding between heterogeneity and intervention effects, yielding more stable, interpretable, and policy-relevant parameter estimates.

6.1. Eigenvalue and Hessian analysis

For our parameter vector $\boldsymbol{\theta} = (\mathcal{R}_0, \nu, t_0, c)$, the Hessian matrix at the maximum likelihood estimate (MLE) represents the local curvature of the negative log-likelihood function. To properly examine parameter identifiability, it is necessary to examine the structure of the Hessian matrix. The eigen decomposition of this Hessian provides information

$$\mathbf{H} = \mathbf{V}\boldsymbol{\Lambda}\mathbf{V}^T, \tag{9}$$

where $\boldsymbol{\Lambda} = \mathrm{diag}(\lambda_1, \lambda_2, \ldots, \lambda_p)$ contains eigenvalues ordered by magnitude ($\lambda_1 \geq \lambda_2 \geq \ldots \geq \lambda_p > 0$) and $\mathbf{V} = [\mathbf{v}_1, \mathbf{v}_2, \ldots, \mathbf{v}_p]$ contains the corresponding eigenvectors.

The eigenvalues indicate how quickly the likelihood function changes when moving in different directions in parameter space:

- *Large eigenvalues*: Directions with high curvature, where parameters are well-constrained.

- *Small eigenvalues*: Directions with low curvature ("flat valley"), where parameters are poorly constrained.

- *Condition number $\kappa = \lambda_1/\lambda_p$*: Indicates numerical stability; large values ($\kappa > 1000$) suggest practical identifiability issues.

We performed an analysis for synthetic single epidemics and then concurrent epidemics which share the same dynamics with a view to alleviating the correlation as we shall see shortly. In our analysis of the Hessian for single-epidemic fits, we consistently observe one eigenvalue significantly smaller than the others, indicating a direction in parameter space with low curvature and thus poor identifiability with a large condition number. However, if two epidemics curves are simultaneously used to compute the Hessian, the condition number is substantially reduced.

The correlation matrix derived from the inverse Hessian,

$$\text{Corr}_{ij} = \frac{(\mathbf{H}^{-1})_{ij}}{\sqrt{(\mathbf{H}^{-1})_{ii}(\mathbf{H}^{-1})_{jj}}}, \tag{10}$$

quantifies the statistical dependencies between parameter estimates.

6.2. Profile likelihood approach for assessing parameter identifiability

The profile likelihood approach offers a practical method to visualize identifiability issues by exploring how the likelihood changes when one parameter is varied while all others are optimized. For a parameter θ_i, the profile likelihood is defined as

$$PL(\theta_i) = \max_{\theta_j, j \neq i} L(\boldsymbol{\theta}). \tag{11}$$

This approach involves fixing one parameter at various values within a plausible range and re-optimizing all other parameters through maximum likelihood estimation. This process generates a curve of maximum log-likelihood values as a function of the fixed parameter, enabling the construction of confidence intervals and revealing structural correlations between parameters.

We applied this method to 200 simulated datasets using the reduced SEIR model with gamma-distributed susceptibility. Each dataset was generated with parameters $\mathcal{R}_0 = 3.0$ (basic reproduction number), $\nu = 1.414$ (coefficient of variation), $t_0 = 15$ days (behavioural change), and $c_1 = 0.3$ ($1-$ intervention strength), then fitted using maximum likelihood estimation. For the two-epidemic scenario, we simultaneously simulated a "baseline" epidemic (initial conditions $\mathsf{E}(0) = 100$, $\mathsf{I}(0) = 40$) and an "auxiliary" epidemic ($\mathsf{E}(0) = 1000$, $\mathsf{I}(0) = 400$) with identical parameters. For each dataset, we profiled all the four parameters and analysed the resulting likelihood profiles, parameter correlations, confidence intervals, and eigenvalue structures of the Hessian matrices. During optimization, we employed parameter transformations (logarithmic for $\mathcal{R}_0$, ν, and t_0; logit transformation for c_1) to ensure parameter constraints were maintained during optimization. Confidence intervals were determined using the chi-square cutoff method, where parameter values yielding likelihood ratio statistics below the threshold defined by $\chi^2_{0.95,1} = 3.84$ were included in the 95% confidence interval.

The profile likelihood analysis was performed as follows:

1. A range of values was defined for each parameter of interest around the MLE corresponding to each parameter.

2. For each fixed value of this parameter, the likelihood was maximized over all other parameters.

3. The resulting likelihood profile was used to determine 95% confidence intervals using the chi-square criterion.

Supplementary Figures S9-S12 show representative profile likelihood curves for all four parameters from a randomly selected sample dataset, comparing the single-epidemic versus two-epidemic approaches.

The profile likelihood curves reveal substantially narrower confidence intervals in the two-epidemic approach compared to the single-epidemic approach across all parameters. This is particularly evident for the coefficient of variation parameter (ν), where the confidence interval width is reduced by approximately 93%, and for the intervention strength parameter (c_1), where the confidence interval narrows from $(0.270, 0.325)$ in the single-epidemic approach to $(0.296, 0.304)$ in the two-epidemic approach, representing a 85.4% reduction in width.

6.3. Parameter estimation accuracy and precision

Table 3 presents the parameter estimation results across all 200 datasets, comparing the single and two-epidemic approaches.

Table 3: Parameter estimates and confidence interval comparisons ($c_1 = 0.3$).

Parameter	Single epidemic		Two epidemics		CI width reduction
	Mean (SD)	CI width	Mean (SD)	CI width	
R_0	3.00 (0.03)	0.090	3.00 (0.01)	0.038	57.6% (2.4×)
ν	1.42 (0.18)	0.571	1.41 (0.01)	0.043	92.5% (13.3×)
t_0	14.98 (0.36)	1.174	15.01 (0.19)	0.667	43.2% (1.8×)
c_1	0.30 (0.02)	0.055	0.30 (0.00)	0.008	86.1% (7.2×)

The most substantial improvement is observed for the coefficient of variation parameter (ν), with a 13.3-fold increase in precision. The 7.2-fold improvement in precision for the intervention strength parameter (c_1) is also noteworthy. These width-reduction improvements can be visualised in Supplementary Figure S13 which displays the 95% confidence intervals of parameter estimates from all the datasets, along with the respective median values.

To further examine the statistical performance of both approaches, we analysed the relative bias and coverage probabilities of the confidence intervals across all 200 datasets, as shown in Supplementary Tables S1 and S2. The results demonstrate

that the two-epidemic approach not only provides more precise estimates but also exhibits lower relative bias for most parameters.

6.4. Numerical stability

To assess numerical stability, we analysed the condition numbers of the Hessian matrices at the maximum likelihood estimates. Table 4 and Supplementary Figure S14 summarize these results.

Table 4: Hessian Matrix Condition Numbers Comparison

Metric	Single epidemic	Two epidemics
Mean	4347.5	59.2
Median	3069.6	59.3
Minimum	376.5	47.7
Maximum	40911.3	69.3
Standard deviation	4703.0	3.2
Relative improvement	73.43× (98.6% reduction)	

The two-epidemic approach exhibits substantially improved numerical stability, with a mean condition number of 59.3 compared to 3069.6 for the single-epidemic approach. This represents an almost 98.6% improvement, indicating that the two-epidemic approach produces a better-conditioned optimization problem. The substantially lower variability in condition numbers (SD of 3.2 versus 4703.0) further demonstrates the consistent numerical stability of the two-epidemic approach across different datasets. For scenarios with condition numbers exceeding 40,000 in the single-epidemic approach, parameters become increasingly difficult to estimate accurately.

6.5. Parameter correlation analysis

We computed pairwise parameter correlations between the 200 estimates to understand how the two-epidemic approach affects parameter identifiability. Figure 8 shows the correlation matrices for both approaches.

While some parameter pairs show reduced correlations, others maintain similar levels, reflecting the complex trade-offs in parameter identifiability. Most importantly, the two-epidemic approach successfully reduces correlations for the parameter pairs that concern this study the most - those that directly impact our ability to separate heterogeneity effects from intervention effects. This provides the mechanistic foundation for the improved precision and identifiability observed throughout this analysis.
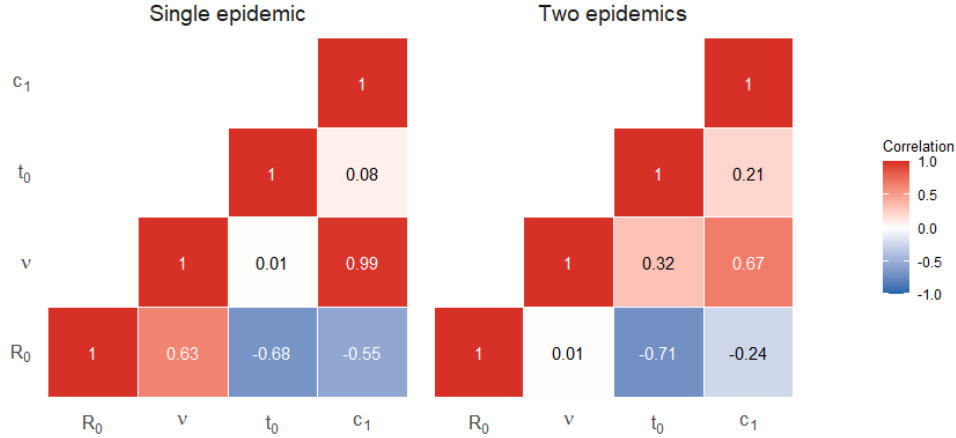
Figure 8: Median parameter correlation heatmaps comparing single-epidemic (left) and two-epidemic (right) approaches. Lower correlations in the two-epidemic approach indicate improved parameter identifiability.

7. Sensitivity to initial conditions and intervention strength

We now examine how the initial conditions of the auxiliary epidemic affect the gain in parameter identifiability relative to the single-epidemic approach. We present results for three values of the intervention parameter ($c_1 = 0.2, 0.3, 0.4$). All other parameters remain fixed as usual: $\mathcal{R}_0 = 3.0$, $\nu = 1.414$, and $t_0 = 15$ days.

Specifically, we simulated two concurrent epidemics: a baseline epidemic with $I(0) = 40$; and an auxiliary epidemic with $I(0) \in \{20, 40, 80, 160, 320, 400\}$. For each scenario, we generated 200 synthetic datasets and analysed parameter correlations using maximum likelihood estimation.

Figures 9, 10, and 11 show how parameter correlations vary with the initial condition of the auxiliary epidemic.

As expected, all correlations tend to decrease as the initial condition of the auxiliary epidemic deviates from that of the baseline. In addition, we see that as the intervention becomes stronger (decreasing c_1), the correlation between $\mathcal{R}_0$ and ν increases, while those between $\mathcal{R}_0$ and t_0 and between ν and c_1 decrease. This effect is especially pronounced in the case of ν-c_1. In the COVID-19 study of Gomes et al. (2022), c_1 was estimated between 0.2 and 0.3, in agreement with the empirical study
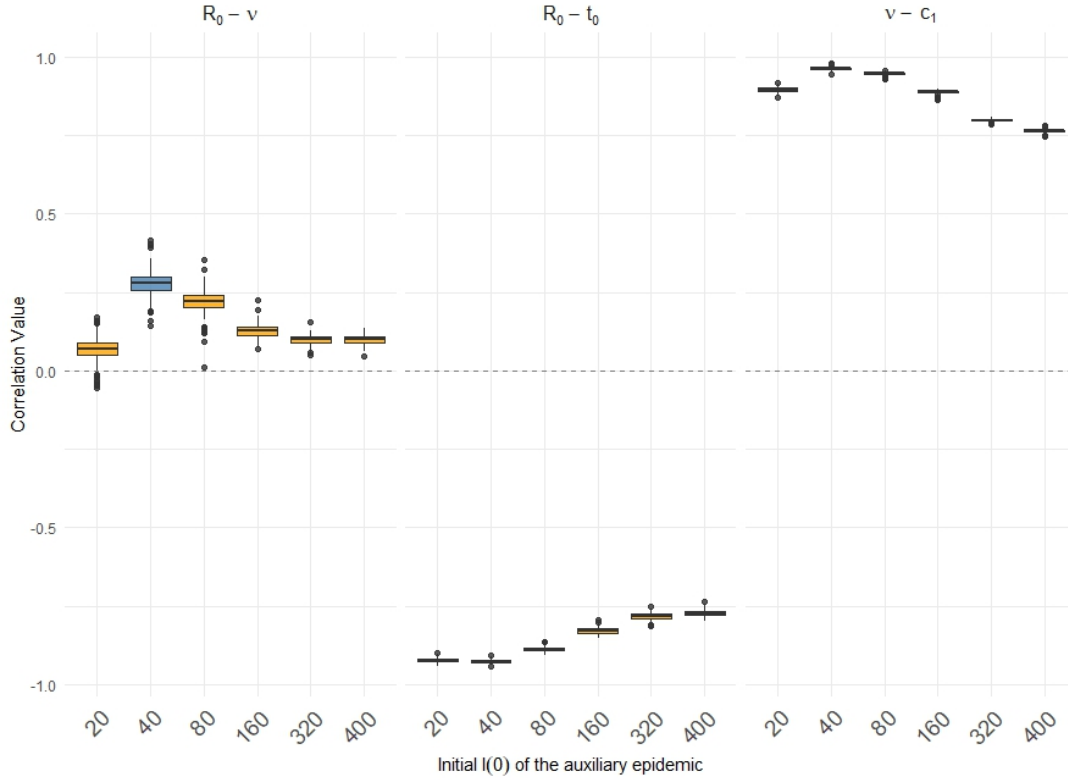
Figure 9: Correlation distributions in terms of the initial condition of the auxiliary epidemic ($I(0) \in \{20, 40, 80, 160, 320, 400\}$) for intervention parameter $c_1 = 0.4$. The baseline epidemic is initiated with $I(0) = 40$ in all cases. Cases where baseline and auxiliary epidemics coincide (i.e., have the same initial conditions) are marked in blue.

of Jarvis et al. (2020), which happens to be favourable regime from the identifiability perspective.

8. Prediction of epidemic trajectories

Understanding the uncertainty in parameter estimates is crucial for predicting the potential course of outbreaks. Using the estimated parameters for both homogeneous and heterogeneous models, we constructed prediction intervals and examined the models' forecasting capabilities. We used a multivariate normal distribution for generating parameter sets that preserve the correlations between parameter estimates. This approach allows us to assess not only how well models fit observed data, but crucially, how reliably they predict future epidemic trajectories.
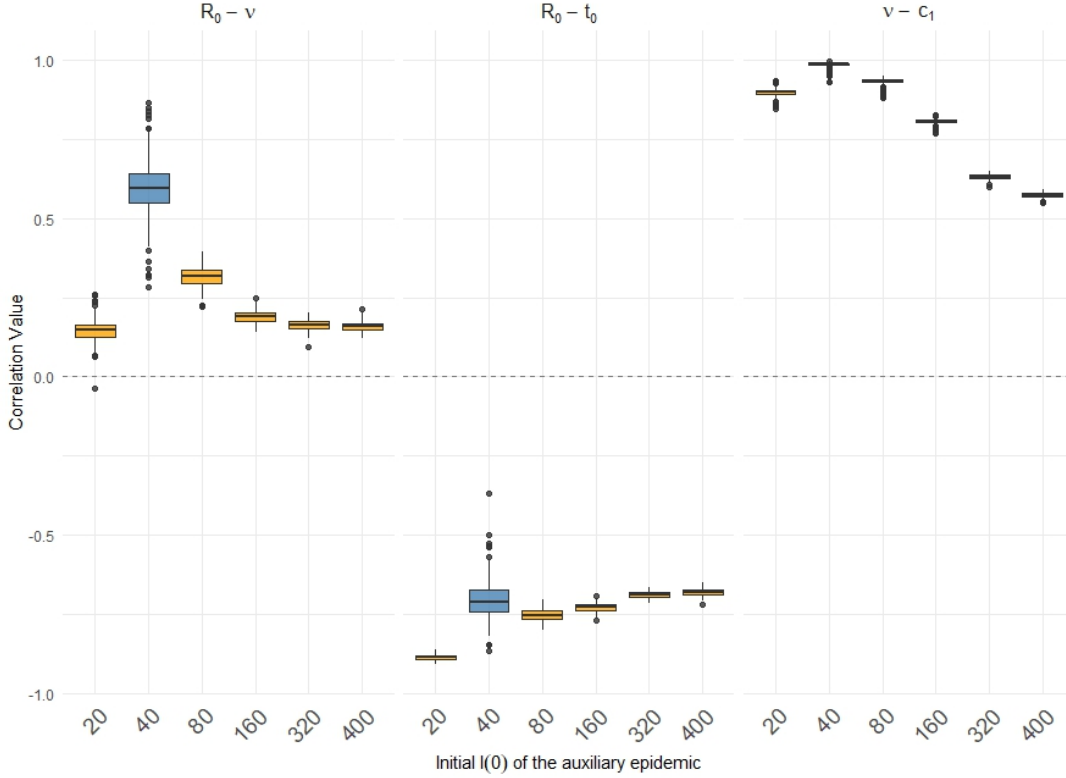
Figure 10: Correlation distributions in terms of the initial condition of the auxiliary epidemic ($I(0) \in \{20, 40, 80, 160, 320, 400\}$) for intervention parameter $c_1 = 0.3$. The baseline epidemic is initiated with $I(0) = 40$ in all cases. Cases where baseline and auxiliary epidemics coincide (i.e., have the same initial conditions) are marked in blue.

Figure 12 shows the prediction results for Case I(b), where data were generated from a homogeneous population subject to NPIs. During the fitting period (days 1-100), both models perform similarly, accurately capturing the trajectory of the epidemic with relatively narrow prediction intervals. This is consistent with our parameter estimation results in Table 2, where both models recovered unbiased estimates of the reproduction number $\mathcal{R}_0 = 3$ and intervention strength $c_1 = 0.3$.

Interestingly, even in the forecasting period (days 100-250), both models maintain similar trajectories despite the heterogeneous model estimating a small, non-zero coefficient of variation ($\hat{\nu} = 0.201$ instead of the true value of 0). The homogeneous model's forecast is visually undistinguishable from the "ground truth" (dashed black line), while the heterogeneous' is only slight below. The wide confidence band for the heterogeneous model is mainly due to the uncertainty in the estimation of CV,
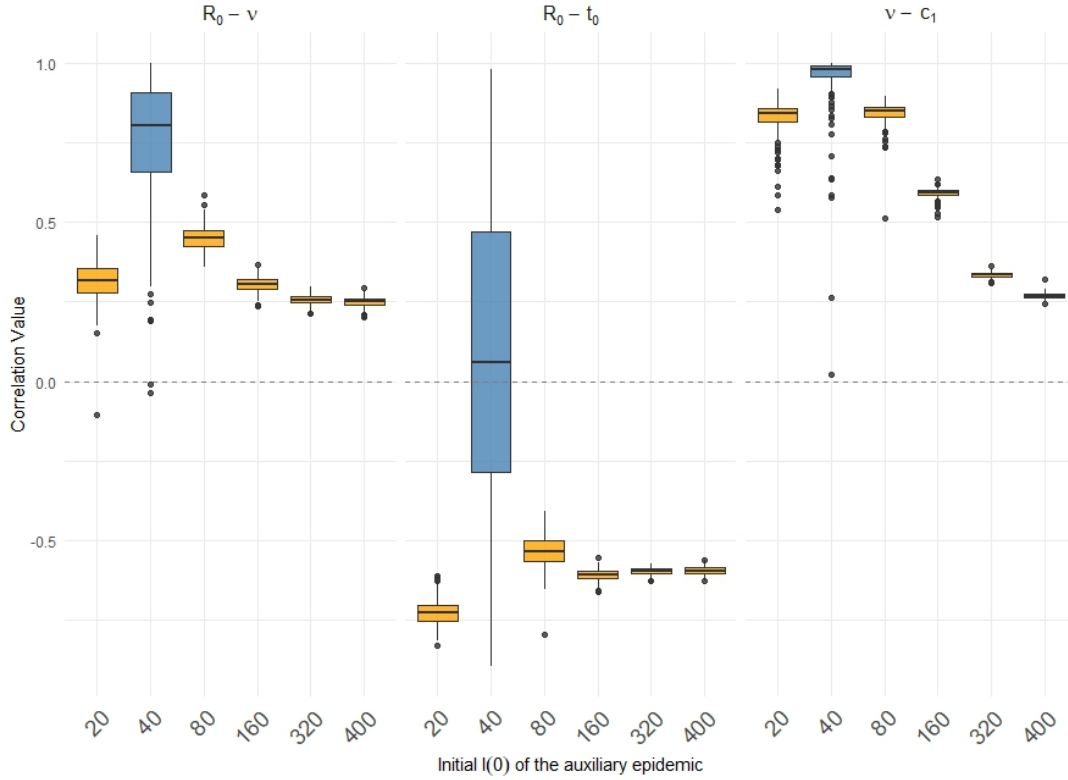
Figure 11: Correlation distributions in terms of the initial condition of the auxiliary epidemic ($I(0) \in \{20, 40, 80, 160, 320, 400\}$) for intervention parameter $c_1 = 0.2$. The baseline epidemic is initiated with $I(0) = 40$ in all cases. Cases where baseline and auxiliary epidemics coincide (i.e., have the same initial conditions) are marked in blue.

which has a 95% CI of $(0, 04, 0.912)$.

Figure 13 presents a contrasting scenario for Case II(b), where data were generated from a heterogeneous population subject to NPIs. While both models fit the initial 100 days of data reasonably well, their forecasts diverge substantially. The homogeneous model predicts a massive second wave with peak daily cases approaching 2750 — nearly four times higher than the first wave. In contrast, the heterogeneous model predicts a much more modest second wave with peak daily cases of approximately between 300 and 1000.
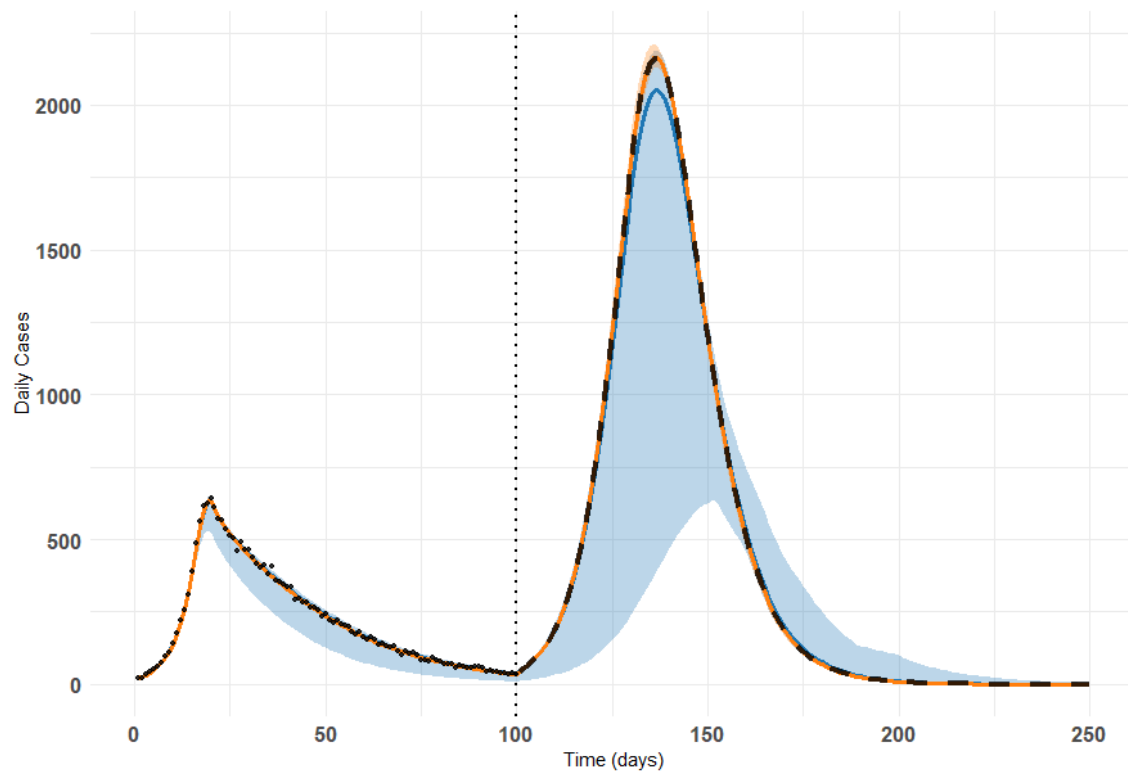
Figure 12: Prediction trajectories for Case I(b): Homogeneous data with NPIs. Models were fitted to the first 100 days of data (black dots) and then used to forecast the next 150 days. Heterogeneous model fit (blue); homogeneous model fit (orange). The dashed black line represents the "true" trajectory generated with the assumed parameter values.
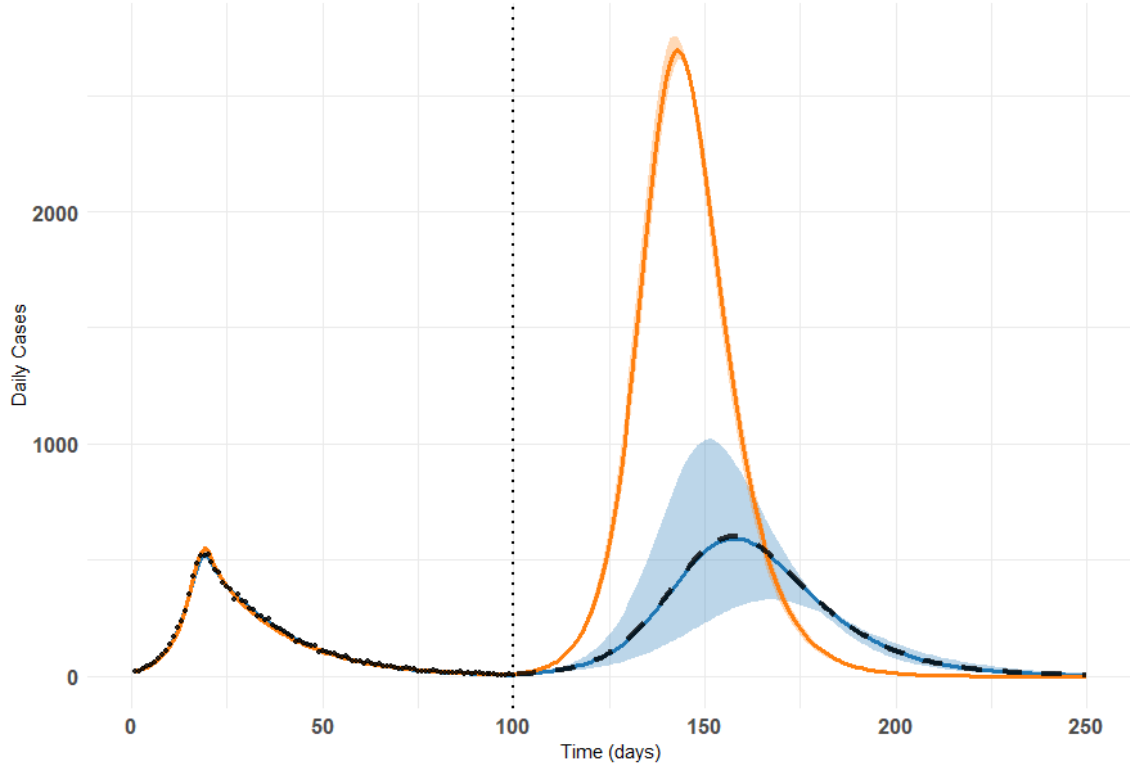
Figure 13: Prediction trajectories for Case II(b): Heterogeneous data with NPIs. Models were fitted to the first 100 days of data (black dots) and then used to forecast the next 150 days. Heterogeneous model fit (blue); homogeneous model fit (orange). The dashed black line represents the "true" trajectory generated with the assumed parameter values.

When compared to the "ground truth" (dashed black line), it is evident that the heterogeneous model's forecast is remarkably accurate, while the homogeneous model's prediction represents a substantial overestimation. This stark difference in forecasting performance stems from the homogeneous model's inability to account for the depletion of highly susceptible individuals during the first wave, which naturally limits the severity of subsequent waves. Instead, the homogeneous model attributes the flattening of the curve in the first wave primarily to intervention effects ($\hat{c}_1 = 0.24$ instead of the true value of 0.30), incorrectly suggesting that a larger proportion of the population remains susceptible for the second wave.

The wider prediction intervals for the heterogeneous model reflect greater uncertainty in the estimation of CV ($\hat{\nu} = 1.406$ with 95% CI of $(1.157, 1.768)$), but despite this uncertainty, even the upper bound of its prediction interval remains well below the homogeneous model's median forecast. This underscores that accounting for population heterogeneity is essential not only for accurate parameter estimation but also for reliable forecasting of epidemic trajectories, especially for long-term predictions and scenarios involving multiple epidemic waves.

These findings have profound implications for public health planning. Homogeneous models may lead to substantial overestimation of disease burden in subsequent waves, potentially resulting in unnecessarily stringent or prolonged interventions. Conversely, models that properly account for heterogeneity provide more realistic forecasts that can inform more proportionate public health responses.

9. Conclusions

In this study, we conducted the first systematic investigation of parameter identifiability for the SEIR model with inter-individual variation in susceptibility to infection. The work consisted in simulating datasets using a stochastic version of the model with strategically chosen parameter values - with or without heterogeneity, with or without non-pharmaceutical interventions - and then conducting maximum likelihood estimation to assess how well we could retrieve the assumed parameter values. The key findings are as follows:

- Model parameters are generally estimated accurately, but there is a tendency for high uncertainty in the estimated CV of susceptibility when fitting to data that included NPIs.

- Strong correlations among pairs of estimated parameters are generally apparent, whether heterogeneity is included as a parameter or not, indicating potential issues with identifiability.

- The issues highlighted above can be practically eliminated by simultaneously fitting two epidemic trajectories with some shared parameters.

The strategy of fitting multiple epidemics with shared parameters to gain identifiability has been used successfully in real-world investigations (e.g., White et al. (2007); Aguas et al. (2008); Gomes et al. (2022)), but a systematic study of the strengths of the approach was, to our knowledge, lacking. We hope that the significance of the results reported here will motivate others to conduct such investigation for other systems, and apply the approach in real settings.

Competing interests

No competing interest is declared.

Author contributions statement

All authors conceived the study, implemented the models, analysed the results and wrote the paper.

Data and code availability

Computer code used to simulate epidemics and estimate model parameters is available from https://github.com/ibrahimStrathclyde/On-the-simultaneous–inference–of–epidemic-susceptibility-distributions-and-NPI

Appendix A. Supplementary material

Supplementary material related to this article can be found online at...

References

Aguas, R., White, L.J., Snow, R.W., Gomes, M.G.M., 2008. Prospects for malaria eradication in sub-saharan africa. PLoS ONE 3, e1767.

Anderson, D., Burnham, K., 2004. Model selection and multi-model inference. Second. NY: Springer-Verlag 63, 10.

Ayabina, P., Sevil, H., Kleczkowski, A., Gomes, M.G.M., 2025. A note on metapopulation models. Journal of Theoretical Biology 613, 112213. doi:https://doi.org/10.1016/j.jtbi.2025.112213.

Ball, F., 1985. Deterministic and stochastic epidemics with several kinds of susceptibles. Advances in applied probability 17, 1–22.

Britton, T., Ball, F., Trapman, P., 2020. A mathematical model reveals the influence of population heterogeneity on herd immunity to sars-cov-2. Science 369, 846–849.

Diekmann, O., Heesterbeek, H., Britton, T., 2013. Mathematical Tools for Understanding Infectious Diseases. Princeton Series in Theoretical and Computational Biology, Princeton University Press.

Gart, J.J., 1968. The mathematical analysis of an epidemic with two kinds of susceptibles. Biometrics , 557–566.

Gart, J.J., 1972. The statistical analysis of chain-binomial epidemic models with several kinds of susceptibles. Biometrics , 921–930.

Gelman, A., Carlin, J.B., Stern, H.S., Dunson, D.B., Vehtari, A., Rubin, D.B., 2013. Bayesian Data Analysis. Chapman and Hall/CRC.

Gomes, M.G.M., Ferreira, M.U., Corder, R.M., King, J.G., Souto-Maior, C., Penha-Gonçalves, C., Gonçalves, G., Chikina, M., Pegden, W., Aguas, R., 2022. Individual variation in susceptibility or exposure to sars-cov-2 lowers the herd immunity threshold. Journal of Theoretical Biology 540, 111063.

Jarvis, C.I., Van Zandvoort, K., Gimma, A., Prem, K., Klepac, P., Rubin, G.J., Edmunds, W.J., 2020. Quantifying the impact of physical distance measures on the transmission of covid-19 in the uk. BMC medicine 18, 124.

Katriel, G., 2012. The size of epidemics in populations with heterogeneous susceptibility. Journal of mathematical biology 65, 237–262.

Keeling, M.J., Rohani, P., 2002. Estimating spatial coupling in epidemiological systems: a mechanistic approach. Ecology Letters 5, 20–29. URL: http://doi.wiley.com/10.1046/j.1461-0248.2002.00268.x, doi:10.1046/j.1461-0248.2002.00268.x.

Kerr, C.C., Stuart, R.M., Mistry, D., Abeysuriya, R.G., Rosenfeld, K., Hart, G.R., Núñez, R.C., Cohen, J.A., Selvaraj, P., Hagedorn, B., George, L., Jastrzebski, M., Izzo, A.S., Fowler, G., Palmer, A., Delport, D., Scott, N., Kelly, S.L., Bennette, C.S., Wagner, B.G., Chang, S.T., Oron, A.P., Wenger, E.A., Panovska-Griffiths, J., Famulare, M., Klein, D.J., 2021. Covasim: An agent-based model of COVID-19 dynamics and interventions. PLoS Computational Biology 17. doi:10.1371/journal.pcbi.1009149.

Lauer, S.A., Grantz, K.H., Bi, Q., Jones, F.K., Zheng, Q., Meredith, H.R., Azman, A.S., Reich, N.G., Lessler, J., 2020. The incubation period of coronavirus disease 2019 (covid-19) from publicly reported confirmed cases: estimation and application. Annals of internal medicine 172, 577–582.

Lehmann, E.L., Casella, G., 2006. Theory of point estimation. Springer Science & Business Media.

Li, Q., Guan, X., Wu, P., Wang, X., Zhou, L., Tong, Y., Ren, R., Leung, K.S., Lau, E.H., Wong, J.Y., et al., 2020. Early transmission dynamics in wuhan, china, of novel coronavirus–infected pneumonia. New England journal of medicine 382, 1199–1207.

McAloon, C., Collins, Á., Hunt, K., Barber, A., Byrne, A.W., Butler, F., Casey, M., Griffin, J., Lane, E., McEvoy, D., et al., 2020. Incubation period of covid-19: a rapid systematic review and meta-analysis of observational research. BMJ open 10, e039652.

McKendrick, A., 1940. The dynamics of crowd infection. Edinburgh Medical Journal 47, 117.

Montalbán, A., Corder, R., Gomes, M.G.M., 2022. Herd immunity under individual variation and reinfection. Journal of Mathematical Biology 85, 2.

Neipel, J., Bauermann, J., Bo, S., Harmon, T., Jülicher, F., 2020. Power-law population heterogeneity governs epidemic waves. PloS one 15, e0239678.

Nishiura, H., Linton, N.M., Akhmetzhanov, A.R., 2020. Serial interval of novel coronavirus (covid-19) infections. International journal of infectious diseases 93, 284–286.

Novozhilov, A.S., 2008. On the spread of epidemics in a closed heterogeneous population. Mathematical Biosciences 215, 177–185. URL: https://www.sciencedirect.com/science/article/pii/S0025556408001211, doi:https://doi.org/10.1016/j.mbs.2008.07.010.

Robert, C.P., Casella, G., 1999. Monte Carlo statistical methods. volume 2. Springer.

Rose, C., Medford, A.J., Goldsmith, C.F., Vegge, T., Weitz, J.S., Peterson, A.A., 2021. Heterogeneity in susceptibility dictates the order of epidemic models. Journal of Theoretical Biology 528, 110839. URL: https://www.sciencedirect.com/science/article/pii/S0022519321002587, doi:https://doi.org/10.1016/j.jtbi.2021.110839.

Tkachenko, A.V., Maslov, S., Elbanna, A., Goldenfeld, N., 2021. Time-dependent heterogeneity leads to transient suppression of the covid-19 epidemic, not herd immunity. Proceedings of the National Academy of Sciences USA 118, e2015972118.

White, L., Mandl, J., Gomes, M., Bodley-Tickell, A., Cane, P., Perez-Brena, P., Aguilar, J., Siqueira, M., Portes, S., Straliotto, S., Waris, M., Nokes, D., Medley, G., 2007. Understanding the transmission dynamics of respiratory syncytial virus using multiple time series and nested models. Mathematical Biosciences 209, 222–239. doi:https://doi.org/10.1016/j.mbs.2006.08.018.

Wood, S.N., Wit, E.C., McKeigue, P.M., Hu, D., Flood, B., Corcoran, L., Jawad, T.A., 2025. Some statistical aspects of the covid-19 response. Journal of the Royal Statistical Society Series A: Statistics in Society (to appear) .